

The Influence of Chemical Short Range Order on Atomic Diffusion in Al–Ni Melts

S. K. Das and J. Horbach*

Institut für Physik, Johannes Gutenberg–Universität Mainz, 55099 Mainz, Germany

M. M. Koza

⁴*Institut Laue–Langevin, 38042 Grenoble, France*

S. Mavila Chatoth and A. Meyer[†]

Physik Department E 13, Technische Universität München, 85747 Garching, Germany

(Dated: September 16, 2018)

Abstract

We use inelastic neutron scattering and molecular dynamics (MD) simulation to investigate the chemical short range order (CSRO), visible through prepeaks in the structure factors, and its relation to self diffusion in Al–Ni melts. As a function of composition at 1795 K Ni self diffusion coefficients from experiment and simulation exhibit a non-linear dependence with a pronounced increase on the Al–rich side. This comes along with a change in CSRO with increasing Al content that is related to a more dense packing of the atoms in Ni–rich Al–Ni systems.

PACS numbers: 61.20.-p,61.20.Ja,61.12.-q

*Electronic address: horbach@uni-mainz.de

†Electronic address: ameyer@ph.tum.de

In hard-sphere like metallic liquids mass transport is strongly connected to the packing fraction of the atoms [1, 2, 3]. However, in liquid Al–Ni [4], Al–Fe [5, 6] and glass forming Al rich alloys [7] the structure clearly deviates from a random hard-sphere packing and exhibits a chemical short range order (CSRO) [8]. As was shown in a neutron diffraction experiment on liquid Al₈₀Ni₂₀ [4], CSRO manifests itself in a prepeak in the static partial structure factors at an intermediate lengthscale around 1.8 Å⁻¹. In this paper, we study the composition dependence of the CSRO in Al–Ni melts and show how it affects the diffusion dynamics in this alloy. To address this issue, we performed inelastic neutron scattering experiments and molecular dynamics (MD) simulations.

Al–Ni alloys were prepared by arc melting of pure elements under a purified Argon atmosphere. The corresponding solidus and liquidus temperatures were measured with differential scanning calorimetry and found to be in excellent agreement with the phase diagram [9]. For the neutron time-of-flight experiment on the IN6 spectrometer of the Institut Laue-Langevin, thin-walled Al₂O₃ containers were used that provide a hollow cylindrical sample geometry of 22 mm in diameter and a thickness of 1.2 mm for the Al rich samples, and 0.6 mm for the Al₂₅Ni₇₅ sample. An incident neutron wavelength of $\lambda = 5.1$ Å yielded an energy resolution of $\delta E \simeq 92 \mu\text{eV}$ (FWHM) and an accessible wave number range at zero energy transfer of $q = 0.4 - 2.0$ Å⁻¹. Al_{100-x}Ni_x alloys were measured above their liquidus temperatures at 1525 K and at 1795 K for $x = 10, 20, 23, 30$, and at 1795 K for $x = 38, 75$ compositions.

The scattering law $S(q, \omega)$ was obtained by normalization to a vanadium standard, correction for self absorption and container scattering, and interpolation to constant wave numbers q . Further, $S(q, \omega)$ was symmetrized with respect to the energy transfer $\hbar\omega$ by means of the detailed balance factor. Fourier transformation of $S(q, \omega)$, deconvolution of the instrumental resolution, and normalization with the value at $t = 0$ gave the time correlation function $\Phi(q, t)$. For times above $\simeq 1$ ps, $\Phi(q, t)$ shows an $\exp(-q^2 D_q t)$ decay to zero. Towards small q incoherent scattering on the Ni atoms dominates the signal and the q -dependent diffusivity D_q becomes constant. Thus, Ni self diffusion coefficients D could be derived on an absolute scale [3, 10].

In order to model the interaction between the atoms in the MD simulation, we used a potential of the embedded atom type that was recently derived by Mishin *et al.* [11]. The simulations were done at 1795 K and 1525 K for different Al–Ni compositions. The systems

consist of 1500 particles in each case. First standard Monte–Carlo (MC) simulations in the NpT ensemble [12] were used to fully equilibrate the systems at zero pressure and to generate five independent configurations for MD simulations in the microcanonical ensemble. In the latter case, Newton’s equations of motion were integrated with the velocity Verlet algorithm using a time step of 1.0 fs. From the MD trajectories the structure factors and diffusion constants were determined [13].

By integrating the scattering law $S(q, \omega)$ over the quasielastic line inelastic neutron scattering also gives access to structural information on intermediate length scales. Fig. 1 displays the integral over the quasielastic line (denoted by $S_{\text{qu}}(q)$ in the following) for the Al-Ni melts at 1795 K. For clarity a constant that approximates the incoherent scattering on the Ni atoms has been subtracted. For Al-rich alloys the spectra exhibit a prepeak that is increasing with increasing Ni content and that shifts from $\simeq 1.6 \text{ \AA}^{-1}$ in $\text{Al}_{80}\text{Ni}_{20}$ to $\simeq 1.8 \text{ \AA}^{-1}$ in $\text{Al}_{62}\text{Ni}_{38}$. In $\text{Al}_{90}\text{Ni}_{10}$ nearly no prepeak is visible anymore. As compared to the data at 1795 K, the quasielastic structure factors measured at 1525 K do not reveal a measurable shift in the peak positions and the intensities in the maxima of the prepeaks exhibit a $\simeq 20\%$ increase which can be accounted for by the increased Debye-Waller factor. On the Ni rich side the $\text{Al}_{25}\text{Ni}_{75}$ $S_{\text{qu}}(q)$ also exhibits a prepeak. This prepeak is much broader, though, and has its maximum at $\simeq 1.5 \text{ \AA}^{-1}$.

Fig. 2 shows the measured Ni self diffusion coefficients as a function of composition at 1525 K and at 1795 K. At 1795 K values range from $3.95 \pm 0.10 \times 10^{-9} \text{ m}^2 \text{ s}^{-1}$ in $\text{Al}_{25}\text{Ni}_{75}$ to $10.05 \pm 0.11 \times 10^{-9} \text{ m}^2 \text{ s}^{-1}$ in $\text{Al}_{90}\text{Ni}_{10}$. The Ni self diffusion coefficient in $\text{Al}_{25}\text{Ni}_{75}$ is equal within error bars to the value in pure liquid Ni with $D = 3.80 \pm 0.06 \times 10^{-9} \text{ m}^2 \text{ s}^{-1}$ [3]. Substitution of 25 % Ni by Al does not affect the diffusion coefficient significantly. In contrast, on the Al rich side diffusion coefficients show a pronounced increase with increasing Al content.

The temperature and concentration dependence of the measured diffusion coefficients are well reproduced by the ones of the MD simulation: There is an overall 20% agreement with the experimental data (Fig. 2). From the inset of Fig. 2 we see also that in our simulation the ratio $D_{\text{Al}}^*/D_{\text{Ni}}^*$ does not depend on temperature in the considered temperature range (here the star means that diffusion constants from the simulation are considered). Note that the diffusion constants, that were obtained in a recent simulation study by Asta *et al.* [14] using different EAM potentials, are a factor 2–3 higher than those obtained in our simulation, but

also display a pronounced non-linear behavior as a function of composition. As we shall see in the following, the non-linear behavior of the diffusion coefficients is reflected in structural changes that can be understood from the detailed information provided by the simulation.

Fig. 3 displays the $S_n(q) = \frac{1}{N_{\text{Al}}b_{\text{Al}}^2 + N_{\text{Ni}}b_{\text{Ni}}^2} \sum_{k,l}^N b_k b_l \langle e^{i\mathbf{q} \cdot (\mathbf{r}_k - \mathbf{r}_l)} \rangle$, with \mathbf{r}_k being the position of the k 'th particle. N_α , $\alpha \in \text{Al, Ni}$, denotes the number of atoms of type α , and $b_{\text{Al}} = 0.3449 \cdot 10^{-12}$ cm and $b_{\text{Ni}} = 1.03 \cdot 10^{-12}$ cm are respectively the neutron scattering lengths of Al and Ni. As Fig. 3 shows, also a prepeak is observed in the simulation which is located at slightly smaller q for the Al rich systems whereas for $\text{Al}_{30}\text{Ni}_{70}$ the prepeak is at a slightly larger q than expected from the experiment. However, in particular for the Al rich systems a similar behavior as in the experiment is found, i.e., with increasing Al concentration, the prepeak becomes broader, its amplitude decreases and its location shifts to smaller q . We note that $S_{\text{qu}}(q)$ and $S_n(q)$ are *different* quantities, since $S_{\text{qu}}(q)$ is also affected by the q dependence of the Debye-Waller factor. Moreover, $S_{\text{qu}}(q)$ contains a mixture of incoherent and coherent contributions that cannot be disentangled from each other. Thus, one should compare only the *relative* intensities of the peaks in the experimental $S_{\text{qu}}(q)$.

Also shown in Fig. 3 is the main peak which indicates repeating units of neighboring atoms. The location of this peak moves to higher q towards the Ni rich systems which is due to the fact that with increasing Ni concentration the packing density of the atoms increases [16]. This can be inferred from the inset of Fig. 3 which shows the atomic volume V_a as found in the simulation in comparison to experimental data [15]. Note that we get an overall 5% agreement with the experiment over the whole Al concentration range. The nonlinear behavior of V_a is strongly correlated with the nonlinear behavior of the diffusion constants as a result of the CSRO.

$S_{\text{qu}}(q)$ and $S_n(q)$ are total structure factors which are in binary systems linear combinations of three partial structure factors. In order to understand the CSRO that is present in Al-Ni melts one has to consider these partial structure factors defined by $S_{\alpha\beta}(q) = \frac{1}{\sqrt{N_\alpha N_\beta}} \sum_{k_\alpha=1}^{N_\alpha} \sum_{l_\beta=1}^{N_\beta} \langle \exp(i\mathbf{q} \cdot (\mathbf{r}_{k_\alpha} - \mathbf{r}_{l_\beta})) \rangle$, where the indices k_α and l_β correspond to particles of type α and β , respectively. In Fig. 4 the different $S_{\alpha\beta}(q)$ are shown again at $T = 1525$ K for Al rich compositions, for a 50:50 mixture, and for the Ni rich composition $\text{Al}_{30}\text{Ni}_{70}$. The emergence of a prepeak in $S_{\alpha\beta}(q)$ indicates that there are repeating structural units involving next-nearest $\alpha\beta$ neighbors which are built in inhomogeneously into the structure. As we see in Fig. 4, no prepeak emerges in $S_{\text{AlAl}}(q)$ for the Al rich

compositions but the main peak moves slightly to higher q with decreasing Al concentration. By further decreasing the Al concentration a prepeak evolves that moves to smaller q . As a result a double peak structure is observed in $S_{\text{AlAl}}(q)$ for $\text{Al}_{30}\text{Ni}_{70}$ with maxima at $q_1 = 1.8 \text{ \AA}^{-1}$ and $q_2 = 3.0 \text{ \AA}^{-1}$. In $S_{\text{AlNi}}(q)$ a prepeak with a negative amplitude is visible at all Al concentration and, as in the Al–Al correlations, this prepeak moves to smaller q with decreasing Al concentration. The negative amplitude of the prepeak in $S_{\text{AlNi}}(q)$ is due to the avoidance of corresponding Al–Ni distances. Also in $S_{\text{NiNi}}(q)$ a prepeak is present at all concentrations. This prepeak broadens with increasing Al concentration while its location remains essentially constant. In $\text{Al}_{30}\text{Ni}_{70}$ the main peak is at the same location in the three different partial structure factors, namely around $q = 3.0 \text{ \AA}^{-1}$.

The picture provided by the simulation is as follows: In the Ni rich systems the minority species Al is built into the structure such that the distance between repeated Al–Al units corresponds to that of repeated Ni–Ni units [16] whereas towards the Al rich systems the distance between repeated Al–Al units becomes larger without a significant change in the distance between repeated Ni–Ni units. All this explains the nonlinear behavior of the atomic volume and, since it indicates a nonlinear behavior of the packing of the atoms upon a change of the composition, it demonstrates that the nonlinear increase of the diffusion constants upon increasing Al content is essentially a packing effect. Of course, this packing argument does not explain the deviation of $D_{\text{Al}}^*/D_{\text{Ni}}^*$ from one for the Ni rich systems. The understanding of this feature requires a microscopic theory.

In conclusion, an investigation of Al–Ni melts using inelastic neutron scattering and MD simulation has shed light onto the nonlinear composition dependence of the diffusion constants and its relation to chemical short range order visible through a prepeak in the structure factor. We confirm the finding for other hard-sphere like metallic melts [3] that the transport in these systems is strongly affected by packing effects although the interactions between the atoms depend strongly on chemical details.

We are grateful to Kurt Binder for stimulating discussion. The authors acknowledge financial support by the Deutsche Forschungsgemeinschaft (SPP Phasenumwandlungen in mehrkomponentigen Schmelzen) under Grant No. Bi314/18 and Me1958/2. One of the authors (J. H.) acknowledges the support of the DFG under Grant No. HO 2231/2.

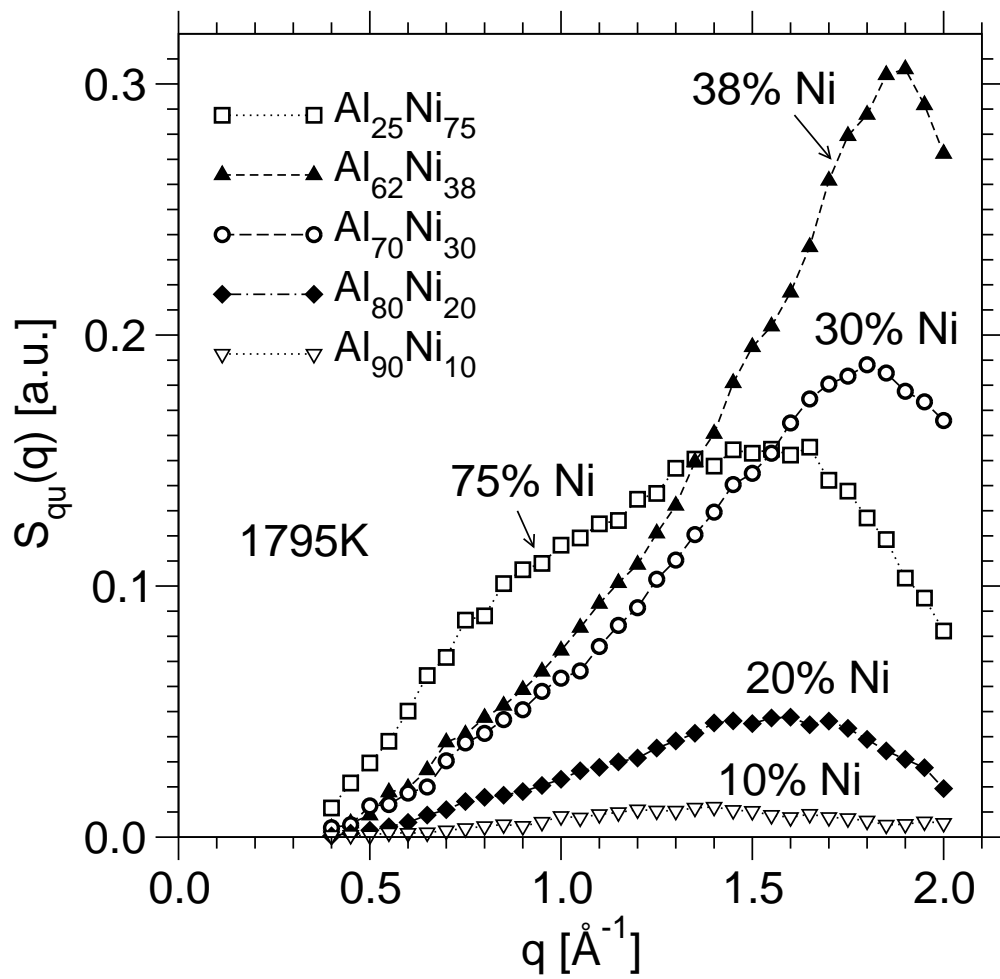
-
- [1] P. Protopapas, H. C. Andersen, and N. A. D. Parlee, *J. Chem. Phys.* **59**, 15 (1973).
- [2] G. Foffi, W. Götze, F. Sciortino, P. Tartaglia, and Th. Voigtmann, *Phys. Rev. Lett.* **91**, 085701 (2003).
- [3] S. Mavila Chathoth, A. Meyer, M. M. Koza, and F. Yuranji, *Appl. Phys. Lett.* (in press).
- [4] M. Maret, T. Pomme, A. Pasturel, and P. Chieux, *Phys. Rev. B* **42**, 1598 (1990).
- [5] Q. Jingyu, B. Xiufang, S. I. Sliusarenko, and W. Weimin, *J. Phys.: Condens. Matter* **10**, 1211 (1998).
- [6] A. Il'inskii, S. Slyusarenko, O. Slukhovskii, I. Kaban, and W. Hoyer, *Mater. Sci. Engin. A* **325**, 98 (2002).
- [7] Z. Lin, W. Youshi, B. Xiufang, L. Hui, W. Weimin, L. Jingguo, and L. Ning, *J. Phys. Condens. Matter* **11**, 7959 (1999).
- [8] T. Egami in F. E. Luborsky (ed.), *Amorphous Metallic Alloys* (Butterworths, London, 1983).
- [9] B. Predel, edited by O. Madelung, *Phase Equilibria of Binary Alloys* (Springer, Berlin, 2003).
- [10] A. Meyer, *Phys. Rev. B* **66**, 134205 (2002).
- [11] Y. Mishin, M. J. Mehl, and D. A. Papaconstantopoulos, *Phys. Rev. B* **65**, 224114 (2002).
- [12] D. P. Landau and K. Binder, *A Guide to Monte Carlo Simulations in Statistical Physics* (Cambridge University Press, Cambridge, 2000).
- [13] K. Binder, J. Horbach, W. Kob, W. Paul, and F. Varnik, *J. Phys.: Condens. Matter* **16**, S429 (2004).
- [14] M. Asta, D. Morgan, J. J. Hoyt, B. Sadigh, J. D. Althoff, D. de Fontaine, and S. M. Foiles, *Phys. Rev. B* **59**, 14271 (1999).
- [15] G. D. Ayushina, E. S. Levin, and P. V. Geld, *Russ. J. Phys. Chem.* **43**, 2756 (1969).
- [16] The location of the first peak in the corresponding pair correlation functions $g_{\alpha\beta}(r)$ does not depend on the Al–Ni composition.

FIG. 1: Quasielastic coherent structure factor $S_{\text{qu}}(q)$ at intermediate q of Al–Ni melts at 1795 K as obtained by inelastic neutron scattering (see text).

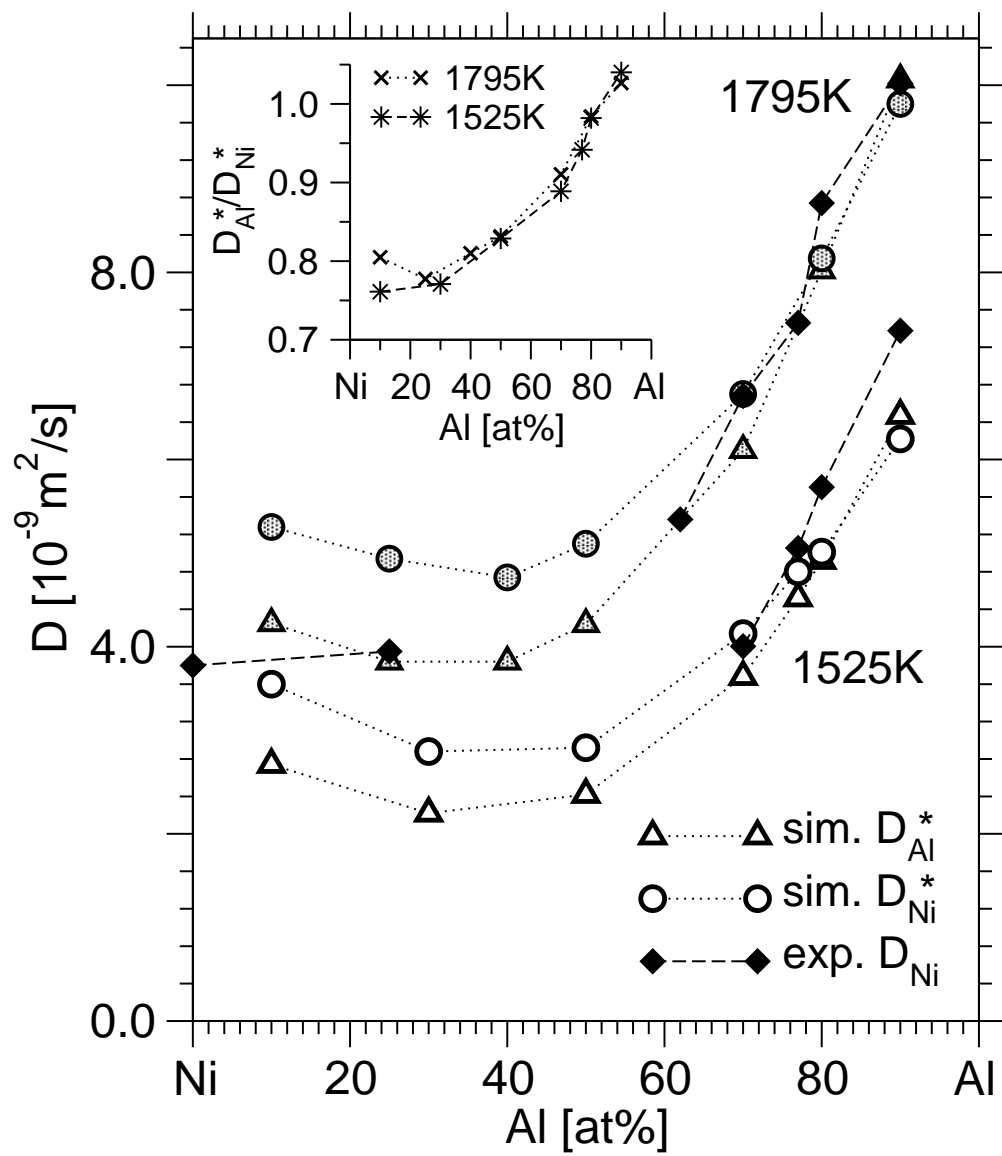
FIG. 2: Diffusion coefficients at 1795 K and at 1525 K as a function of the aluminium concentration from simulation and neutron scattering. The broken lines are guides to the eye. Inset: Ratio of Al and Ni self diffusion coefficients from simulation. Note that the diffusion constants from the simulation are decorated by a star.

FIG. 3: Structure factors $S_{\text{n}}(q)$ of Al–Ni melts as calculated from the partial structure factors of the simulation weighted with the neutron scattering length. Inset: Atomic volume from the simulation compared to experimental data from Ref. [15] as a function of composition.

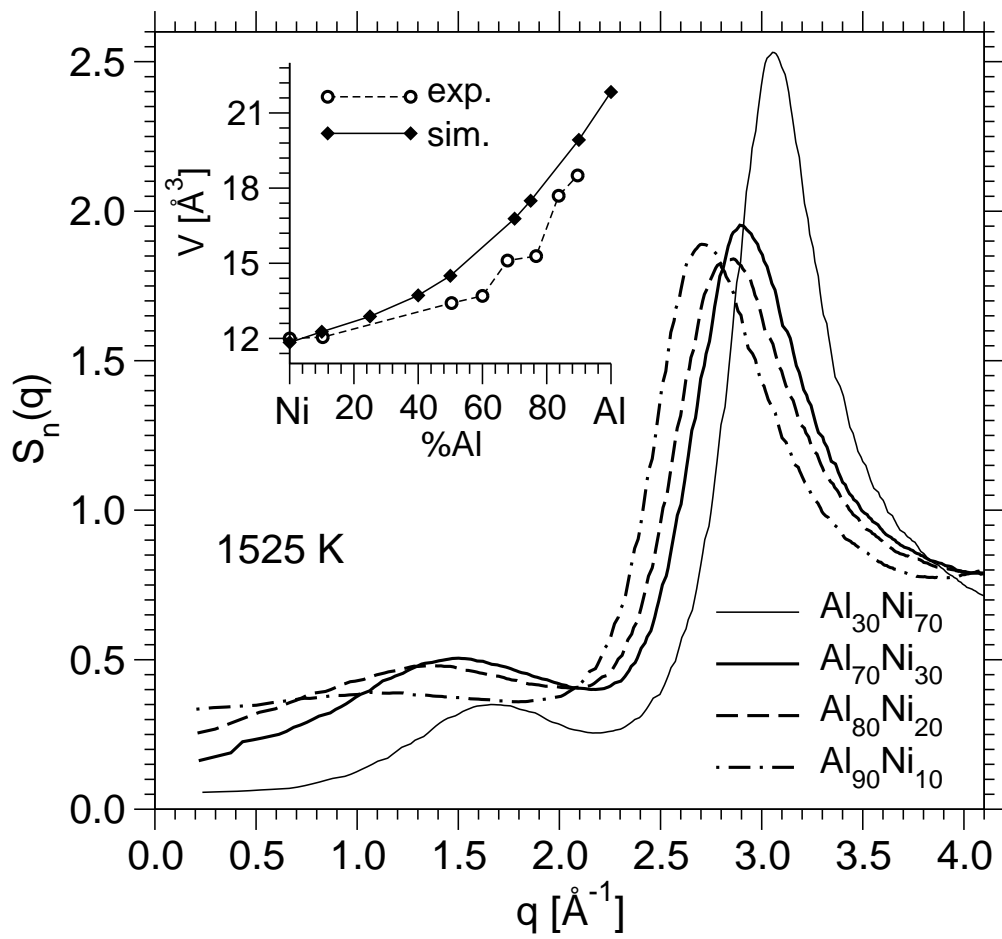
FIG. 4: Partial structure factors $S_{\alpha\beta}(q)$ of Al–Ni melts as determined by the simulation at 1525 K. a) $S_{\text{AlAl}}(q)$, b) $S_{\text{AlNi}}(q)$, and c) $S_{\text{NiNi}}(q)$.



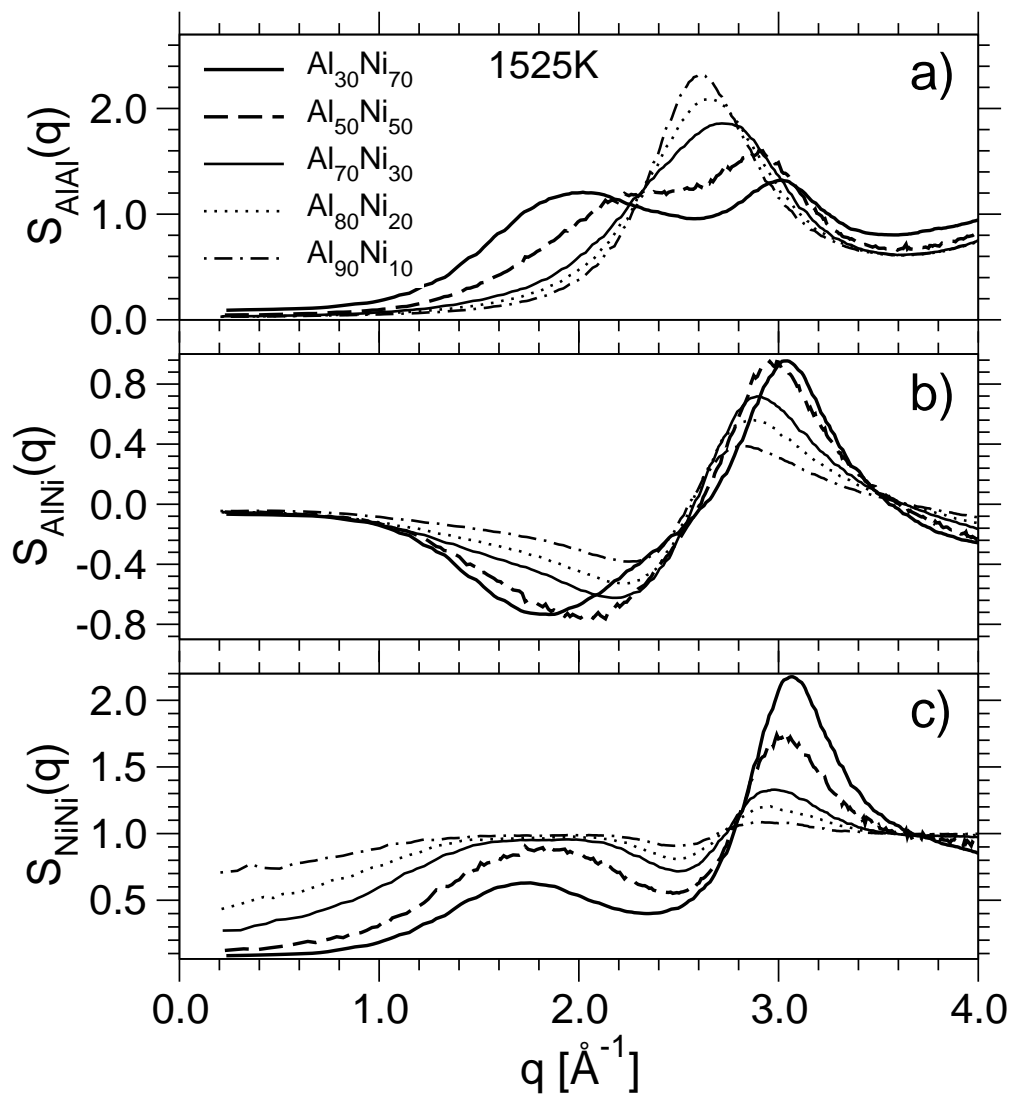
Das et al., Figure 1



Das et al., Figure 2



Das et al., Figure 3



Das et al., Figure 4